

Advances in pulsed phase thermography

by X. Maldague^{1,2}, J.-P. Couturier¹, S. Marinetti¹, A. Salerno², D. Wu²

¹Electrical and Computing Engineering Department, University Laval,
Quebec City, Quebec, Canada G1K 7P4;

²IKP - Universität Stuttgart, Pfaffenwaldring 32, D-70569 Stuttgart (Vaihingen) Germany

Abstract

A succinct depth analysis of Pulsed Phase Thermography (PPT) is presented in this paper. Some theory is presented as well including some comparisons with modulated (or lockin) thermography (MT).

1. Introduction

Pulsed phase thermography (PPT) is a novel way to process infrared thermal images acquired in the pulsed (or transient) heating mode. In the first report about this new technique [1], it was demonstrated that it shares advantages of both conventional pulsed infrared thermography (PT) and modulated (or lockin) thermography (MT). In this paper, it is reported that a frequency analysis of phase images obtained in PPT is also possible enabling depth-tuning capabilities. Experiments will be presented from both pulsed phase thermography and modulated approaches.

2. Theoretical aspects

In order to introduce PPT concepts, lets first recall some specific principles of both MT and PT. Notice that in the subsequent discussions, it is assumed that recording of temperature signals is done in two dimensions (image format), as for surface heating.

In MT, a single frequency is tested in the stationary regime and the thermal response of the sample is analysed to obtain magnitude and phase images (the specimen is submitted to a sinusoidal temperature modulation and its stationary response is also described by a sinusoidal regime). In most nondestructive evaluation applications, phase ϕ images are of particular interest [2]. In PT, the analysis generally proceeds by computing the maximum thermal contrast image from images recorded during the temperature decay, just after the end of the heating pulse [3, p. 122].

In PPT deployment, the specimen is pulse-heated as in PT and the mix of frequencies of the thermal waves launched into the specimen is unscrambled by performing the Fourier transform of the temperature decay on a pixel by pixel basis: this enables computation of phase images. For each pixel (i, j) , the temporal decay $f(x)$ is extracted from the image sequence (where x is the index in the image sequence). Next, from $f(x)$, the discrete Fourier transform $F(u)$ is computed (u being the frequency variable). Finally, from the real $R(u)$ and imaginary $I(u)$ components of $F(u)$, the phase is computed using the well known formula $\phi(u) = \text{atan}\{I(u)/R(u)\}$.

In the first report about PPT [1], the interest was focused on the maximum phase image (ϕ_{\max}) obtained by recording, for every pixel, the maximum numerical value of ϕ regardless of the frequency value u . This was done by analogy with the conventional contrast processing approach where the maximum contrast is often the prime interest [3]. Obviously, it is also possible to explore the various frequencies u . However an important point to remember is that the analysis in PPT is performed in the transient mode while in MT, the signal is recorded in the stationary mode. Nevertheless, it was shown in [1] that PPT shares many of the attractive features of MT and thus, the possibility to proceed with a frequency analysis of the PPT phase images looks attractive.

Such a frequency study leads to $\phi(u)$ computations. In the Fourier analysis, the range of frequencies spans from 0 to $1/\Delta x$ where Δx is the sampling rate of the infrared imaging apparatus. The frequency increment Δu is given by $1/N\Delta x$, where N is the number of images in the recorded decay sequence. For example, if 50 images are recorded at an interval of 33.3 ms ($f = 30$ Hz, NTSC video standard), the range of frequencies spans from 0 to 30 Hz ($= 1/\Delta x = N\Delta u$) in 0.60 Hz frequency increments. Table 1 provides a few values of Δx , N , Δu .

table 1: Relations between acquisition frequency f , sampling rate Δx , number of samples N and frequency increments Δu .

frequency f (Hz)	Δx (ms)	N	Δu (Hz)
0.25	4000	50	0.005
		500	0.0005
1	1000	50	0.02
		500	0.002
25	40	50	0.50
		500	0.05
30	33	50	0.6
		500	0.06
54	19	50	1.08
		500	0.108
300	3	50	6.00
		500	0.60

As seen, from table 1, in order to record quick thermal events in high thermal conductivity specimens (such as aluminum), it is required to have a fast pace recording equipment (such as the 300 Hz Santa Barbara or Cedip infrared FPA - focal plane array - camera capable to provide high Δu values). On the other hand, it is possible to go to very low frequencies with slow recording equipment such as with conventional scanning imagers operating in 25 or 30 Hz and for which infrared images can be grabbed at even slower pace. For instance in some experiments described later, a frequency of 0.005 Hz was used (table 1) to probe deeper into the specimen. In fact, it is recalled that the depth range of phase image [4] is roughly given by the thermal diffusion length μ [m]:

$$\mu = \sqrt{2k/\omega\rho c} \tag{1}$$

with thermal conductivity k [$\text{W m}^{-1} \text{C}^{-1}$], density ρ [kg m^{-3}], specific heat c [$\text{Jkg}^{-1}\text{C}^{-1}$]. Low frequencies enable deep probing under the surface while high frequencies are restricted to shallow probing. These well known aspects of MT will be demonstrated in the case of PPT in the next section.

3. Experimental results

Two different kinds of experimental apparatus were used to obtain the results described in this section. One equipment is dedicated to MT and is based around an Agema 900 infrared camera (long wave: 8-12 μm , maximum recording rate: 15 images per second) with a Unix-based workstation (Agema Thermovision system controller), the lockin option and software from the same company. We will refer to this system as the 'Agema apparatus'. The other apparatus is based on a Cincinnati Electronics 160 FPA camera (short wave: 2-5 μm , maximum recording rate: 54 images per second, 20° lens) with a workstation-based computer (Sun microsystem Sparc 4) and with dedicated software. We will refer to this system as the 'FPA apparatus'. The heating system used is either composed of two heating lamps of 1000 W (electric power) with back reflector or two high power flashes (15 ms duration, 6.4 KJ) with back reflector.

The first specimen is a plastic plate with front surface covered with a high emissivity paint (~0.9). On the back face of the specimen, an inclined 6.4 mm width slot was milled with a variable depth from 1 to 3 mm under the front surface. The specimen was pulse-heated for 15 s and infrared images were recorded with the FPA apparatus. A PPT analysis was performed to compute various phase images at different frequencies ($N=50$ samples, $f=0.25$ Hz, $\Delta x=4$ s, $\Delta u=0.005$ Hz). Figure 1 shows various $\phi(u)$ images with $u=0.04, 0.025, 0.015, 0.01$ Hz respectively from (a) to (d), corresponding to frequency samples number 8, 5, 3 and 2 in the Fourier spectrum (e.g.: 2×0.005 Hz = 0.01 Hz).

Recalling eq. (1), the following approximate depth values are obtained for the plastic specimen (table 2).

table 2: Probing depth as function of frequency for the plastic specimen, using eq. (1).

frequency (Hz)	depth (mm)
0.04	1.7
0.025	2.2
0.015	2.8
0.01	3.5

Comparing the values of table 2 with images of figure 1, it is clear that an agreement is present since for instance at $u=0.01$ Hz, the deepest part of the slot is visible (3 mm) while at $u = 0.04$ Hz, just half is visible in the ϕ image (~ 2 mm). This is an interesting result which opens somehow the possibility to compute depth of subsurface artifacts by scanning the frequency u in the $\phi(u)$ images.

The second specimen is a graphite-epoxy plate with two-embedded Teflon® implants of 10 mm in diameter located respectively about 2 and 3 mm under the front surface. The specimen was tested using both methods: PPT (pulsed phase thermography) with the FPA apparatus and the flashes, and MT (modulated or lockin thermography) with the Agema apparatus and the lamps. figure 2 shows the results for both PPT (a and b) and (MT (c and d).

With the PPT approach, the specimen was pulse-heated for 15 ms with the following parameters ($N= 50$ samples, $f = 1$ Hz, $\Delta x = 1$ s, $\Delta u = 0.02$ Hz), the images were recorded for 50 s. With the MT approach, slow modulations were used (0.12 Hz \leftrightarrow 8.3 s per cycle and 0.06 Hz \leftrightarrow 16.7 s per cycle), the experiment was repeated at both frequencies and we had to wait for the stationary heating regime to establish, for a total experiment length of about 80 s.

Different frequencies were tested in order to demonstrate the depth-tuning capability of the phase ϕ images: 0.12 (MT) and 0.2 (PPT) Hz for the close-to-surface defect and 0.06 (MT) and 0.04 (PPT) Hz for the deeper defect. Recalling eq. (1), the following approximate depth values are obtained for the graphite-epoxy specimen (table 3).

table 3: Probing depth as function of frequency for the graphite-epoxy specimen, using eq. (1).

frequency (Hz)	depth (mm)
0.12	2
0.20	1.6
0.06	3
0.04	3.6

Comparing the values of table 3 with images of figure 2, it is clear that an agreement is present since for instance at fast frequencies ($u = 0.12$ or $u = 0.2$ Hz), only the shallow defect appears while at slower frequencies the deepest defect appears strongly. On this figure, it is important to point out that the fields of view and sample positions are different for both cameras. Interestingly, some features such as the "structure" close to the shallow defect appears both in PPT and MT images (a and c). Its origin is unknown. It is perhaps due to an epoxy displacement caused by the presence of the Teflon® implant nearby. Notice also the dead pixel in the FPA camera (white spot on top of images a) and b) and also the superior spatial resolution of the FPA camera (look at the defect edges, especially the shallow one).

Computation time needed to obtain phase ϕ images is close to 10 s in the case of the Agema apparatus (MT) while it takes about 7 minutes per image in the case of the FPA apparatus (PPT). It should be mentioned that for the PPT case no particular care was taken to optimize the code (the program is written in "C" language) and that parallel hardware implementation or DSP (digital signal processing) board should enhance the cadence (work is pursued in this direction).

4. Conclusion

In this paper, the theory of the frequency analysis in PPT approach was presented while experimental results demonstrated the possibility of such frequency analysis. Moreover, a comparison made between PPT and MT experiments recorded over the same specimen leads to very similar results confirming the close relationship between PPT and MT. Finally, it was also shown that the frequency tuning capability of PPT phase image enables some sort of depth evaluation using the well known thermal diffusion length equation. PPT appears thus to be an attractive addition to pulsed (or transient) thermography.

5. Acknowledgments

The support of the Alexander von Humboldt (AvH) Foundation of Germany (Bonn) and of the Natural Sciences and Engineering Research Council of Canada are kindly acknowledged. X. Maldague is a Fellow of the AvH. Author Salerno acknowledges the support of the Foundation BLANCEFLOR Boncompagni-Ludovisi Née Bildt for granting him a Fellowship. The authors are grateful to German BMBF for support of research on Lock-in thermography (Project Nr. 03N8006B0). Finally, the authors also appreciate the efficient cooperation with AGEMA.

REFERENCES

- [1] MALDAGUE (X.), MARINETTI (S.). - *Pulsed Phase Infrared Thermography*. J. Appl. Phys., 79, 2694-2698 (1996)
- [2] BUSSE (G.), WU (D.), KARPEN (W.). - *Thermal wave imaging with phase sensitive modulated thermography*. J. Appl. Phys., 71, 3962-3965 (1992)
- [3] MALDAGUE (X.). - *Nondestructive evaluation of materials by infrared thermography*. London, Springer-Verlag, 224 p. (1993)
- [4] BUSSE (G.). - *Nondestructive evaluation of polymer materials*. NDT & E Int'l, 27, 253-262 (1994)

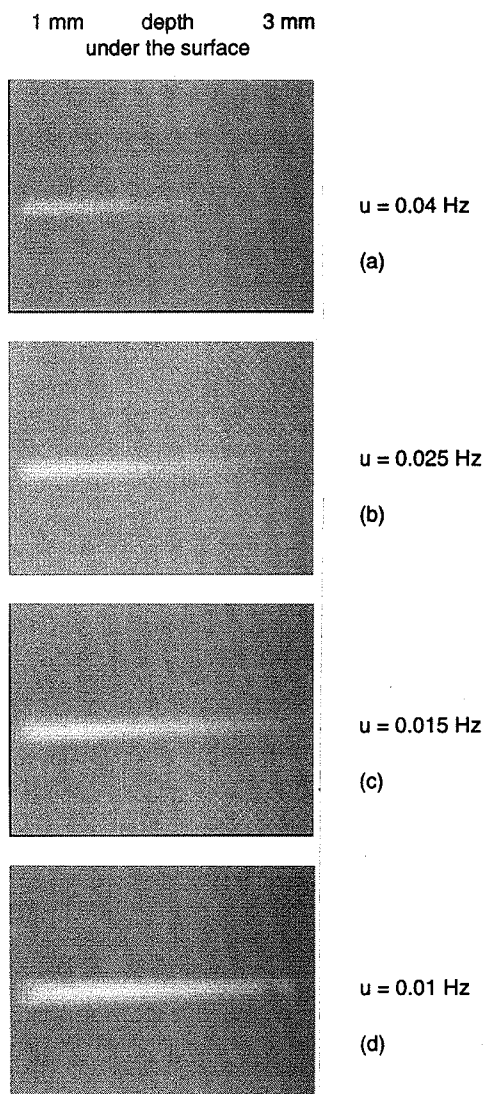


figure 1 Phase images obtained with the PPT approach at various frequencies over a plastic specimen with an inclined slot of 6.4 mm width and of variable depth as shown.

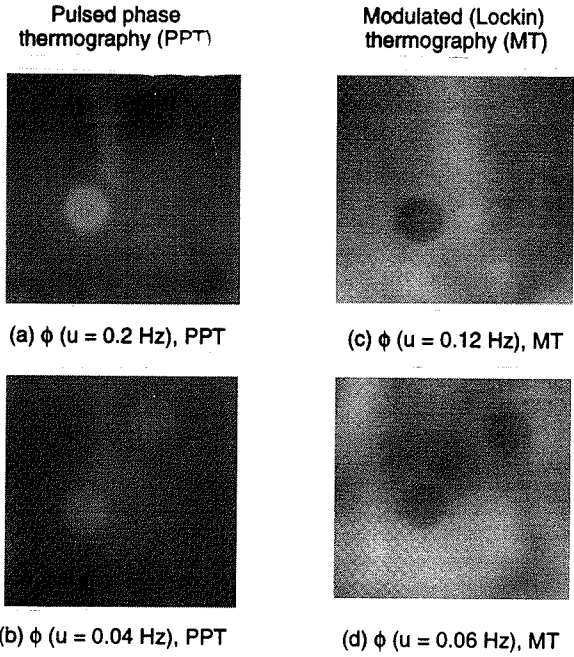


figure 2 Phase images obtained with both PPT (left) and MT (right) approach at various frequencies over a graphite epoxy plate with two-embedded Teflon® implants of 10 mm in diameter located at about 2 and 3 mm under the front surface (different image sizes and operating distances).